# Cells

**VA Sethuraman, AZ Weber, and JW Weidner,** Lawrence Berkeley National Laboratory, Berkeley, CA, USA, and University of South Carolina, Columbia, SC, USA



## Introduction

Proton-exchange membrane fuel cells (PEMFCs) operating on gaseous hydrogen and oxygen are electrochemical energy conversion devices that directly convert hydrogen's chemical energy into electrical energy. In a PEMFC, hydrogen and oxygen combine electrochemically to produce water, power, and waste heat. This direct energy conversion circumvents most of the intermediate steps of producing heat and mechanical work common to majority of power generation methods. As a result, PEMFCs are not limited by the thermodynamic limitations of conventional heat engines, such as Carnot efficiency, and are able to generate high power densities, and thus are potentially attractive for light-duty transportation applications. Additionally, because of the absence of chemical combustion involving carbonaceous fuels, PEMFCs powered by pure hydrogen have minimal environmental impact than most power generators.

The state-of-the-art PEMFC power plant typically consists of (1) a fuel processing unit, which supplies purified hydrogen, (2) a PEMFC stack module, the heart of the power plant, and (3) balance of plant, which includes components that provide water management, thermal management, power conditioning, and other ancillary functions. The PEMFC stack module is in turn made of unit cells that are modularly combined or stacked and are electrically connected to each other. The number of unit cells and the nature of electrical connections between each unit cell are based on the desired output capacity of the PEMFC stack. A unit cell is made of (1) a proton exchange membrane (PEM), (2) anode and cathode electrocatalyst layers placed on either side of the membrane, (3) an electrically conductive gas diffusion layer (GDL) or porous transport layer (PTL) placed next to the catalyst layers, (4) a sealing element, and (5) cell interconnects and/or flow fields that deliver hydrogen and oxygen via gas channels and electrically connect the cells. The anode, cathode, and the membrane constitute the membrane–electrode assembly (MEA) and together with the seal is commonly referred to as a unitized electrode assembly (UEA). The PEM that is in wide use today consists of a polytetrafluoroethylene (PTFE) backbone with perfluorinated-vinyl-polyether side chains containing sulfonic acid end groups (e.g., Nafion®). The anode and cathode catalysts are composite structures consisting of a proton-conducting polymer and a carbon-supported metal catalyst. The GDLs are either carbon paper (e.g., Toray®) or carbon cloth. Figure 1 shows the cross-sectional schematic of a unit cell with a flow field that also serves as a current collector along with the anodic and the cathodic reactions. A three-dimensional view of this unit cell as a repeat unit in a PEMFC stack is shown in Figure 2. A nonporous bipolar plate shown in cross-flow configuration in this figure serves as a flow field for gas distribution as well as a conductor of current from one cell to the next cell.

## Operational Principles of Cell Components

On the anode, hydrogen is oxidized to protons and electrons. The protons move across the membrane (hence the term 'proton exchange membrane') whereas the electrons flow through the external circuit, both toward the cathode, where they combine with oxygen to form water (Figure 1). This flow of electrons creates work and is proportional to the load (or resistance) on the external circuit. Because of the direction of the flow of electrons, the polarity of the anode is negative and that of the cathode is positive. These reactions can occur spontaneously at any temperature above absolute zero.

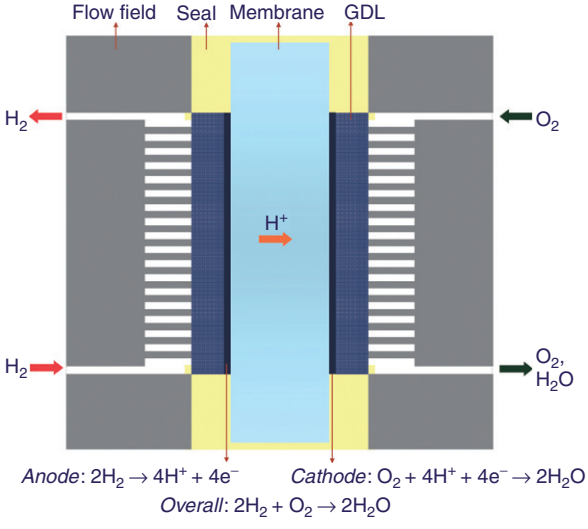


**Figure 1** Cross-sectional view of a proton-exchange membrane (PEM) unit cell. The fuel ($H_2$) is oxidized at the anode catalyst layer (ACL) and the oxidant ($O_2$) is reduced at the cathode. GDL, gas diffusion layer.

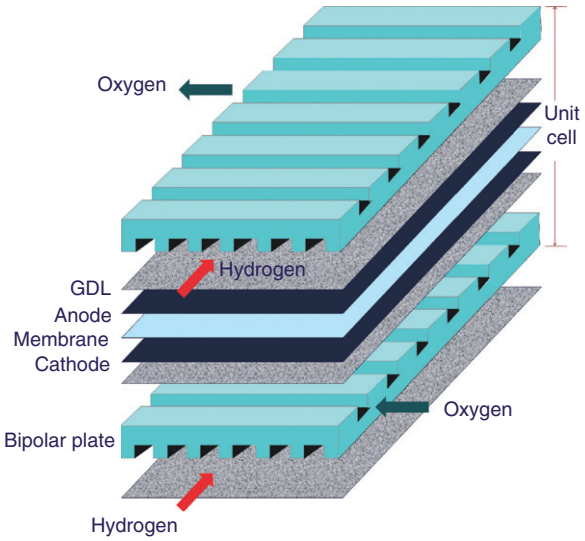


**Figure 2** Three-dimensional schematic of a representative section of a proton-exchange membrane fuel cell (PEMFC) stack shown with cross-flow configuration. The two gas diffusion layers (GDLs), the anode catalyst layer (ACL), proton exchange membrane (PEM), and cathode catalyst layer (CCL) shown here as separate layers constitute a membrane–electrode assembly (MEA). An MEA together with the seal (not shown) constitutes a unitized electrode assembly (UEA). The ACL and CCL are thin layers consisting of catalyst supported on carbon and ionomer. The unit cell repeats itself in a PEMFC stack.

However, PEMFCs are typically operated around 80 °C, where they are most efficient. Although the overall operational principle is simple, the unit cell in itself is a highly integrated system. The unit cell is more than a simple collection of its constituent components because a change in one of them impacts the performance of the others. Each component of the unit cell plays a unique role contributing to the overall operating principle, which is described below.

## Proton Exchange Membrane

The PEM in a PEMFC unit cell serves two important purposes: (1) it keeps the fuel and the oxidant (i.e., hydrogen and oxygen) from mixing and reacting chemically and (2) it serves as the solid polymer electrolyte and selectively transports the protons generated at the anode to the cathode thereby completing the circuit. The functional requirements of PEM include high protonic conductivity; good thermal, mechanical, and chemical stabilities; reasonable operating range (temperature and humidity); low porosity (i.e., low gas transport); and easy manufacturability. The widely used membrane in today's PEMFC is Nafion originally developed by Walther Grot in DuPont in the late 1960s by modifying Teflon®. Nafion ionomer, a subset of polyelectrolytes (i.e., ion-containing polymers), consists of hydrophobic PTFE backbone with perfluorinated-vinyl-polyether side chains containing hydrophilic sulfonic acid end groups. The hydrophobic and the hydrophilic regions come together to form clusters or aggregates and act as physical cross-links. The cluster size depends on water content and increases with water uptake, resulting in swelling. Therefore, Nafion can be said to have the physical and chemical properties of Teflon base material with additional ionic characteristics. These ionomeric polymers are characterized by their equivalent weight defined as the ratio of grams of dry polymer to moles of ion-exchange sites. The lower the equivalent weight, the larger the number of ion-exchange sites. Although a large number of ion-exchange sites are desirable, polymer stability is reduced owing to dissolution at low equivalent weights. Typical commercially available Nafion membranes have an equivalent weight of 1100. The proton conductivity in these ionomers is a strong function of hydration. The proton conductivity mechanism in Nafion is thought to be of two types: (1) Vehicular mechanism, in which the proton is attached to a solvent molecule called vehicle (i.e., $H_3O^+$) and moves at the rate of vehicular diffusion. The net proton transport is governed by vehicle diffusion rates. (2) Grotthuss or hopping mechanism, in which the proton hops from one stationary vehicle to the next vehicle. The solvent reorientation paves the way for $H^+$ conduction and ensures its continuous motion. Because of this, fully hydrated (saturation) conditions result in higher proton conductivities.

These perfluorosulfonic acid membranes were originally developed for the chlor-alkali industry and so the fuel cell environment is relatively mild. The need for high power densities has led to much thinner membranes than those developed for the chlor-alkali industry. For example, Nafion 117 has a thickness of 178 µm (the '7' in '117' refers to a membrane seven thousandths of an inch whereas '11' refers to an equivalent weight of 1100 g $mol^{-1}$). Now the standard for a laboratory unit test cell is Nafion 112, which is 50 µm thick, and unit cells in commercial stacks have membranes thinner than 25 µm. These thinner membranes have less mechanical strength, and this has led several manufacturers to develop composite membranes akin to reinforced Nafion. Another consequence of using thinner membranes is an increase in reactant crossover, which decreases fuel utilization and the cell performance. This is especially problematic in a direct methanol fuel cell because methanol has similar properties as water. Thicker membranes reduce reactant crossover but at the expense of higher resistance and therefore lower power density. Researchers are currently developing composite membranes with the dual properties of high proton conductivity and low reactant crossover.

Although Nafion has been the standard for PEMFCs, the market is demanding alternative operating conditions, which is driving the search for new membranes. For example, the automobile companies would prefer membranes

that are functional at elevated temperatures (>100 °C) and low relative humidities (<25% RH). The former would dramatically reduce the size of the radiator whereas the latter would offer quicker start-up and easier freeze–thaw cycle management. However, it is not possible to maintain adequate membrane water content, and hence acceptable proton conductivity, at higher temperatures without operating at elevated pressures. Elevated pressures introduce additional problems such as a need for an energy-consuming compressor. In addition, the glass transition temperature of Nafion is 111 °C and therefore its mechanical stability is compromised at elevated temperatures.

## Anode and Cathode Catalyst Layers

The anode (ACL) and the cathode catalyst (CCL) layers serve the purpose of (1) catalyzing hydrogen oxidation ($H_2 \rightarrow 2H^+ + 2e^-$) and the oxygen reduction ($O_2 + 4H^+ + 4e^- \rightarrow 2H_2O$) reactions and (2) efficiently transporting the reactants and the products. Typically, the catalyst layers on the anode and cathode are composite structures consisting of the proton-conducting ionomer (e.g., Nafion) and metal catalyst nanoparticles (e.g., platinum) supported on a high surface area carbon (e.g., Vulcan XC 72 or Ketjen Black). Catalyst layer thicknesses vary between 10 and 20 μm depending on catalyst loading levels and ionomer content. Platinum is by far the best catalyst for both the anode and the cathode. However, the choice of the anode catalyst and loading levels also depends on the fuel source. The hydrogen oxidation reaction (HOR) is thought to occur via dissociative adsorption of hydrogen (the limiting step) followed by its oxidation. When operating on pure hydrogen, relatively little platinum (e.g., 0.005 mg cm$^{-2}$) is needed because the HOR is facile (high exchange current density of 1 mA cm$^{-2}$) and the resulting overpotential is small. If the fuel is a reformate (i.e., a mixture of hydrogen, carbon dioxide, nitrogen, and impurities such as carbon monoxide and hydrogen sulfide ($H_2S$) or methanol, then catalysts such as PtRu, PtRh, or PtNi alloys are used to minimize the adverse effect of carbon monoxide poisoning, where carbon monoxide adsorbs on platinum thereby reducing the active sites for hydrogen adsorption. Typically, at least 10 ppm carbon monoxide (and up to 2%) is present in the feed stream. Although platinum can tolerate up to 50 ppm carbon monoxide, bifunctional catalysts such as PtRu and PtAu are required for higher carbon monoxide concentrations. These catalysts require lower overpotential for the formation of $OH^-$ species, which scavenge carbon monoxide species by oxidizing them to carbon dioxide. In addition to using bifunctional catalysts, a small amount (up to 2%) of air or oxygen is fed with the anode fuel stream to promote the chemical oxidation of carbon monoxide on these catalysts.

The oxygen reduction reaction (ORR) is the more limiting reaction in a well-performing fuel cell with exchange current densities as low as $10^{-4}$–$10^{-6}$ mA cm$^{-2}$. Therefore, reducing the activation overpotential for ORR is a crucial factor in improving the fuel cell performance. Increasing the cell temperature and pressure, increasing the reactant concentration (i.e., operating on pure oxygen), and increasing the electrode roughness and the catalyst loading are some of the ways to deal with the performance loss owing to the sluggish ORR kinetics. For example, for a PEMFC fueled with hydrogen and oxygen and operating at 80 °C and 1 atm, the loss owing to the ORR at 0.5 A cm$^{-2}$ can be as high as 160 mV. Currently, the catalyst loading levels on the cathode side are between 0.1 and 0.2 mg cm$^{-2}$. This is a dramatic improvement over loadings in the 1960s, which were about 28 mg cm$^{-2}$. At 2008 prices, this translates into a platinum cost of about $2000 for a 1 kW stack. The twofold decrease in loading levels since then brings platinum costs down to $10 for a similar unit. This is relatively insignificant for an estimated cost of a mass-produced fuel cell subsystem of $325 kW$^{-1}$. However, the Department of Energy's (DoE's) goal of $45 kW$^{-1}$ will require further reduction or elimination in the amount of precious metals.

Although the details vary, the basic structure of the electrode in different PEMFCs is similar. The catalyst particles ~5–20 nm in size are dispersed onto a carbon support (e.g., Vulcan XC-72® Cabot). Smaller particle sizes lead to a larger active area and a better performance per milligram of catalyst loading. However, smaller particles are less stable and so agglomeration of particles occurs over time. Two popular methods are currently practiced in the fabrication of the catalyst layer. In the first method, the carbon-supported catalyst is mixed with an ionomer and is sprayed or electrodeposited onto a porous and conductive material such as carbon cloth or carbon paper. These catalyst-loaded electrodes are then put onto each side of a PEM and hot pressed or steam bonded at a high temperature (between 130 and 150 °C) and at considerable pressures (up to 500 psig) for 2–3 min. The second method involves building the electrodes directly on the PEM. The supported metal catalyst and ionomer mixture is applied to the electrolyte membrane using rolling methods, by spraying or through a process similar to screen printing. Each processing step imparts known and unknown characteristics to the membrane, catalyst layer, and interfaces. Therefore, variations in the processing steps can play as big of a role in performance as variations in materials themselves.

Regardless of the composition of the catalyst, these porous layers contain the sites for charge transfer, and they must also have a dual conduction mechanism. That is, they must conduct protons through the ionomer to complete the ionic path and electrons through the carbon

to complete the electronic path. In addition, gases and water must move easily through these layers. Therefore, an intimate three-phase contact is required for the efficient operation of the unit cell. Finally, one must guard against the case of cell reversal when one of the cells in the fuel cell stack gets starved of fuel. When fuel starvation occurs at the anode, the local anode potential increases causing water electrolysis or carbon oxidation. One way to protect the carbon-based components is to incorporate an additional electrocatalyst in the ACL to sustain the water electrolysis.

## Gas Diffusion Layer

The GDLs or the PTL might play the most critical and least appreciated role of all. As the name implies, the main purpose of the GDL is to distribute the reactants from the gas flow channels uniformly along the active surface of the catalyst layer. In addition, the GDL has to ensure proper transport of product water, electrons, and heat of reaction. It also forms a protective layer over the very thin layer of the catalyst. The GDLs are either carbon paper (e.g., Toray paper) or carbon cloth. The papers are thinner, thus producing a more compact design, whereas the thicker cloths absorb more water and are of superior durability, which simplifies mechanical assembly. Even the GDL is not a simple, uniform structure. Often a microporous layer is added between the main macroporous layer and the catalyst layer. The purpose of this microporous layer is to aid in the distribution of the reacting gases, improve mechanical compatibility between the layers, reduce contact resistance, and improve water management. This microporous layer usually consists of carbon for electrical conductivity and PTFE for hydrophobicity. The in-plane and the through-plane resistivities of the commercial GDLs are in the range of 25–100 $m\Omega\,cm$ and 6–20 $m\Omega\,cm^2$, respectively. The in-plane and the through-plane resistances depend on the microstructure of the GDL. The through-plane resistance dictates the cell resistance and the in-plane resistance affects the reaction uniformity. Further, the role of the GDL in the anode is not usually identical to its role in the cathode. For example, water formed on the cathode must be easily repelled from the catalyst surface to prevent flooding (i.e., liquid water formation). This liquid water blocks catalyst site and prevents oxygen from getting through the catalyst layer. By contrast, the anode must retain some water to keep the membrane from drying out. This is especially true if the anode gas stream is dry. Finally, the placement (such as near the gas inlet/outlet) and the hydrophobicity/hydrophilicity of the microporous layer play a crucial role in water management. For example, the presence of the microporous layer in the anode is more beneficial than in the cathode.

## Seals and Gaskets

The integrated seals and gaskets provide a compact design while performing the primary function of eliminating leaks and overcompression. The thickness and the compressibility of these gaskets dictate compression levels on the GDLs. Also, contaminants from the seals can poison the catalysts or degrade over time. Also, sealing materials are required to separate the gas compartments from each other, to avoid mixing of the fuel hydrogen and the oxidant oxygen, and to prevent leakage and loss of fuel. They also serve additional functions such as electrical insulation and control of stack height. The auto industry with its long history in the design of seals is expected to contribute to PEMFC stack sealing. Silicone and silicon-based elastomers are commonly used as sealing materials in PEMFC stack systems owing to their wide operating temperature (–40 to 300 °C), excellent hardness (20–60), stress relaxation (up to 25% force retained), good electrical resistivity (>1014 $\Omega\,cm$), and dielectric strength (15–17 $kV\,mm^{-1}$). Silicones also have excellent functional properties such as good pressure sealing ability (20–200 kPa), low swelling in PEMFC fluids (< 5%), and low permeability to fuel gases and coolants. However, currently used silicone-based seals, gaskets, and tubing materials fall short of the performance targets. Degraded or substandard seals might cause fuel leaks and may lead to reduced cell voltage owing to mixed potential at the electrodes. Despite their importance, the area of seals and their durability remain the least explored area in PEMFC research.

## Flow Field

The flow field or the bipolar plate serves the following important functions: (1) distribution of reactant gases to the anode and the cathode via gas channels and stack manifolds with minimal parasitic pressure drop; (2) efficient transport of electrons from the anode of one unit cell to the cathode of the neighboring unit cell ensuring constant current in each unit cell; (3) efficient removal of heat generated by the electrochemical reactions; and (4) efficient liquid water storage and transport. Flow fields commonly used in PEMFCs can be porous or nonporous and almost always have channel/land design features. Although most flow fields are nonporous in nature to prevent physical crossover of fuel and oxidant gas feeds, some flow fields known as water transfer plates are porous in nature. They are designed with an extra compartment adjacent to the gas distribution channels that removes excess water through vacuum while also serving as coolant. The channels transport gases to the catalyst layers through the GDL and the land region in contact with the GDL serves to collect current and transport heat. An ideal flow field should serve all of the above-mentioned functions in addition to having

manufacturability and compact design features. Most flow-field designs incorporate one or a combination of the following simple channel configurations: serpentine, parallel, parallel serpentine, mesh, spiral, interdigitated, or foam type. Figure 3 shows some of the basic flow-field design patterns. Each design has its own pros and cons with trade-offs among pressure drops, water removal/uptake capabilities, reactant distribution, and contact resistances.

## Cell Performance and Diagnostics

Most laboratory diagnostics for evaluating the functional characteristics of cell components are performed in a unit cell. The most commonly used unit cell consists of a UEA with 5–25 $cm^2$ active electrode area, modular nonporous flow fields, and end plates. The cell is typically assembled by bolting the end plates together with the cell components (arranged as shown in Figure 2) with an applied torque of 4 Nm at 0.5 Nm intervals ensuring uniform pressure. The assembly is tested for throughput (gas flow) and overboard and crossover leaks. The overboard leak test checks for gas leaks through the seals whereas the crossover leak test checks for physical gas crossover from anode to cathode or vice versa. Both overboard and crossover leak tests are typically done at 5 psig pressure under water. A series of current–voltage (performance or polarization) curves are typically obtained with fully humidified fuel (hydrogen) and oxidant (oxygen) at 70–80 °C as anode and cathode gases, respectively, and at 1 atm as part of the cell incubation procedure. The current–voltage curve is a standard tool for evaluation of a unit cell performance. A simple schematic of the experimental setup used to measure this polarization curve is shown in Figure 4. The cell is usually connected to a variable load bank (or a rheostat) and is operated at either a constant current or a constant potential. The resistance level on the load bank is usually the controlling parameter in both cases. The thermodynamic (or ideal) open-circuit voltage (OCV) of a PEMFC unit cell operating on hydrogen and oxygen is 1.299 V at 298 K. However, mixed potentials caused by gas crossover, internal leakage currents, and impurities result in a measurable OCV (i.e., when $R = \infty$) of ~1 V. A polarization curve is obtained by measuring the current (and hence, the current density) corresponding to a series of cell potentials or vice versa. Figure 5 shows a typical polarization curve of a PEMFC unit cell. If the cell behaves ideally, the measured OCV should equal the ideal Nernstian thermodynamic potential at all current densities. The observed deviation from ideality is a result of several losses and can be broadly grouped into three categories: (1) losses owing to kinetics (active polarization region); (2) losses owing to membrane and other contact resistances (ohmic polarization region); and (3) losses owing to the transport of reactants (concentration polarization region). Although the losses due to the individual contributions are represented as distinct regions in this $V$–$I$ plot, all three losses contribute throughout the entire current range. In brief, the operating voltage of the unit

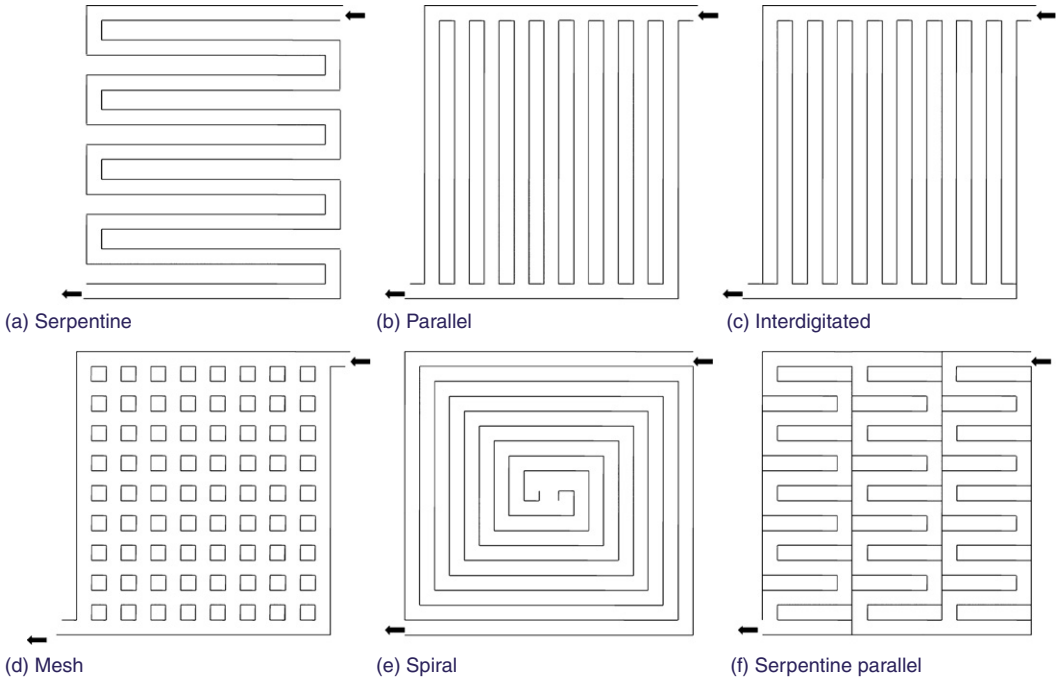


**Figure 3** Schematics of flow-field design patterns. Although basic design patterns are shown, a number of combinations of these design patterns are also used.

cell is a departure from the ideal Nernstian voltage caused by these various losses.

The activation polarization is the voltage lost in the process of initiating the anodic and cathodic electrochemical reactions and therefore dominates at low current densities. Because the rate of an electrochemical reaction is proportional to the exponential of the overpotential, the increase in this activation polarization is significant at lower current densities than at higher currents. The activation polarization is dependent on reaction mechanism, operating parameters such as temperature and pressure, type of catalyst and its morphology, the concentration of hydrogen and oxygen, impurities, and so on. As mentioned earlier, the HOR is a more facile reaction than the ORR and therefore contributes to lower activation polarization loss. All of these dependencies can be engineered to reduce the losses and increase efficiency.

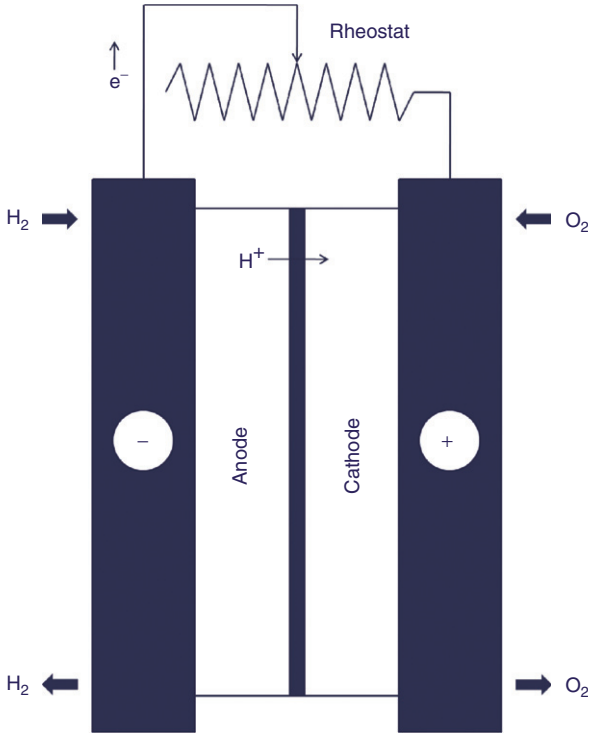


**Figure 4** A simple schematic to show the experimental setup typically used to measure the current–voltage (polarization) curve, and hence the performance, of a proton exchange membrane (PEM) unit cell. The anode and cathode polarities are also shown.

At intermediate current densities, the *V–I* curve is linear and the reduction in the cell voltage is dominated by ohmic polarization. This can be thought of as the sum of ionic and electronic resistances owing to the membrane and other components (e.g., catalyst layers, bipolar plates, GDL) between the anode and the cathode current collectors. Because of very high conductivities exhibited by the catalyst layers, GDL, and the bipolar plates, the membrane contributes predominantly to this ohmic loss. Because the membrane conductivity is highly dependent on the degree of hydration, water management plays a significant role in ohmic losses.

At higher current densities, the system is limited by transport of reactant gases to the catalyst sites and the removal of liquid water out of its point of generation. This can be seen as a knee or a bend in the *V–I* curve at high current densities. Because of this, the power of a fuel cell when plotted against the current density goes through a peak. In addition to the reactant gases and product water transport, the buildup of inert gases and surface blockage by impurities or poisons also contribute

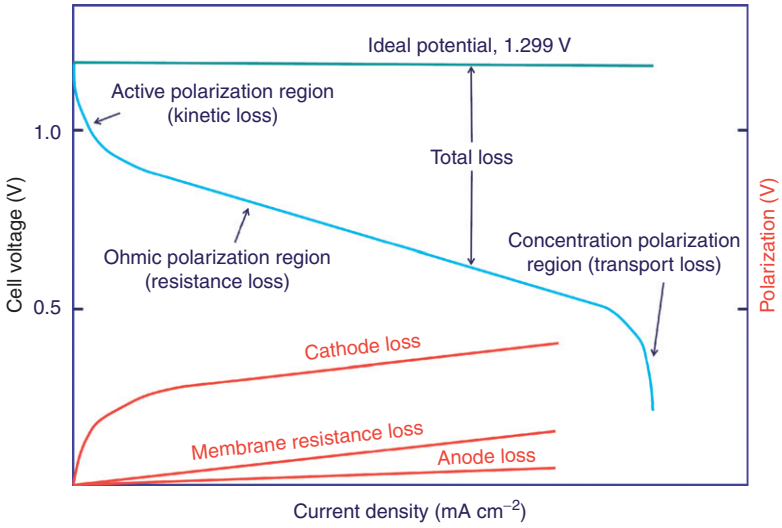


**Figure 5** The voltage–current (*V–I*) curve of a proton-exchange membrane fuel cell (PEMFC) unit cell (blue line) shown along with the ideal *V–I* curve (green line) and polarization losses (red lines) owing to oxygen reduction reaction (ORR) and hydrogen oxidation reaction (HOR) and membrane resistance. Three main losses owing to kinetics, ohmic, and transport are also shown.

**Table 1** Polarization losses owing to various components and diagnostic tools typically used in their estimation

| *Polarization* | *Component* | *Typical value* | *Diagnostic tool* |
|---|---|---|---|
| Kinetic | Anode | 10–20 mV per decade | Half-cell ($H_2/H_2$) |
| | Cathode | 120 mV per decade | RDE |
| Ohmic | Membrane | $l\rho l$, $\rho = 0.1\,\Omega\,m$, $l = 50–175\,\mu m$ | Current interrupt |
| | Bipolar plate | $l\rho l$, $\rho = 0.05\,m\Omega\,m$, $l = 2–5\,mm$ | Four-probe method |
| | Catalyst layer | $l\rho l$, $\rho = 0.2–1\,\Omega\,m$, $l = 5–20\,\mu m$ | EIS, $H_2$ pump |
| | Contact resistances | $IR$, $R = \sim 15–30\,m\Omega\,cm^2$ | – |
| | GDL | $l\rho l$, $\rho = 0.1–0.2\,m\Omega\,m$ | |
| | | $l = 100–300\,\mu m$ | Four-probe method |
| Concentration | $H_2$, $O_2$ | Nernstian | Helox |

EIS, electrochemical impedance spectroscopy; GDL, gas diffusion layer; RDE, rotating disk electrode.

to concentration polarization loss. In addition to the above three polarization losses, gas crossover from either side of the membrane to the other side and electrical short circuits are also detrimental to the performance of the unit cell.

## Diagnostics

Although the polarization curve is the most commonly employed technique for evaluating the overall performance of a unit cell, there are several other diagnostic tools currently in practice to evaluate the performance of the individual cell components.

### *Cyclic voltammetry*

A potential scan (typically between 5 and 20 $mV\,s^{-1}$) is used on the electrode of interest (working electrode) versus the counterelectrode (and reference electrode), usually the catalyst layer or the electrode on the other side of the membrane. The working electrode is usually in contact with an inert gas, whereas the counterelectrode and reference electrode are in contact with dilute hydrogen. Cyclic voltammetry is typically used to measure the electrochemical area (ECA) of the catalyst based on the charge obtained under the hydrogen adsorption and desorption peaks. Electrochemical area is the 'real' catalyst surface area per mass of catalyst (e.g., $m^2\,g^{-1}$). This is essentially the surface area of catalyst that is in contact with both the electrolyte phase and the electronic phase. Electrochemical area is inversely proportional to the size of the particle (e.g., area $= \pi D^2$, mass $= V\rho = \pi D^3\rho/6$, and so ECA $=$ area/mass $= 6/(\rho D)$). Measurement of the active ECA is an important and a fairly common diagnostic technique for evaluating the catalytic activity of platinum or alloy catalysts in the MEA.

Other diagnostic techniques include (1) hydrogen pump experiment to measure the resistance of the ionomer in the catalyst layer, (2) current interrupt technique to measure the ionic resistance of the membrane, (3) the four-probe method to estimate the in-plane and through-plane resistances of the GDL and bipolar plates, (4) electrochemical impedance spectroscopy (EIS) to estimate carbon corrosion and kinetics of a given electrode reaction, (5) Helox experiments to characterize the transport losses, and (6) gas crossover measurements to measure gas permeability across the PEM. Polarization losses owing to various components and diagnostic tools typically used in their estimation are summarized in Table 1. Accelerated durability experiments such as load and humidity, temperature (freeze–thaw) cycling as well as OCV hold experiments are commonly used to evaluate and predict the lifetime capabilities of unit cell components.

## Cell Design and Manufacturing

Design of a PEMFC unit cell strongly depends on its intended application. All UEA producers strive to provide high power density, long and dependable lifetime, low cost, consistent and reliable performance, simplicity of use, and operational flexibility. Unfortunately, these are not mutually exclusive and so there is a continuous trade-off among these goals while continuing to drive down cost. Where that optimum lies depends on the end use of the product as defined by the customer. For example, for stationary applications, durability is the key attribute. These units must run continuously for tens of thousands of hours without fail. Because they are stationary, power density is not as important as lifetime and reliability. Also, these units are large, so the incremental size and cost of additional auxiliary units (e.g., humidifiers, heat exchangers, pumps, and controllers) can be justified if they extend life and minimize maintenance.

For transportation, high power density (i.e., size of the unit) is critical because the units are moving with the load. Therefore, the efficiency of the load plus the fuel cell must be optimized. In addition, durability and flexible operation are also critical design constraints. For example, the load and temperature of these units fluctuate, especially during cold starts or prolonged operation. They must also perform well whether they are being used in the hot sub-Sahara desert or in the middle

of an Arctic winter. For portable applications, size and simplicity must be achieved with dry rather than humidified gas streams. Auxiliary units that can help optimize performance by controlling operating conditions are often not practical. Like unit cells used for transportation, portable applications have varying loads or even no loads for extended periods of time. Therefore, fuel and water management must be maintained even when the cell is not operating. A membrane cannot be allowed to dry out when the fuel cell is not in use or else it will not deliver power when power is demanded. Although cost is always an issue, there are some applications where the consumer will pay premium price for the unique attributes of a fuel cell. For example, the military is willing to pay more than a typical consumer for a device that is quiet, dependable, and has a small thermal signature. As with all industries, the UEA manufacturer must work closely with their customers (i.e., fuel cell manufacturer) and their suppliers (i.e., manufacturers of membranes, catalysts, GDLs, seals) to engineer a UEA that meets the performance requirements and operating conditions of the fuel cell. This requires numerous iterations as UEAs are designed, fabricated, and tested. This process is shown in **Figure 6**.

The process begins with the customer providing performance requirements, design specifications, and operating conditions to the MEA manufacturer. This will include features such as operating temperature, power requirements, size, application (i.e., stationary, transportation, portable), target costs, and fuel and oxygen source. The MEA manufacturer must then choose a set of membranes, catalysts, GDLs, and seals that they feel will meet these specifications. In addition, they must determine how all these layers will be assembled and if there is a need for any interfacial coatings (e.g., microporous layer of a GDL). This requires close consultation with their supplies so that they can get the components with the desired properties. While assessing material properties based on desired fuel cell performance, the MEA manufacturer must also try to drive down their costs by simplifying the manufacturing process without affecting quality. This in itself may affect the selection of materials. For example, the choice of carbon paper or carbon cloth may be dictated by which is more compatible for their assembly process.

Once the materials have been selected and the sequence in which layers are applied has been determined, the MEAs are fabricated, installed in a fuel cell, and tested under the specified operating conditions. These results are compared with the customer's specifications and new sets of materials, in consultation with suppliers, are selected for testing. This interactive process is continued until the customer's requirements are met. Large-scale manufacturing of the MEA follows, and if problems arise here, the iterative process could start over.

What makes this interactive process so involved is that a change in one layer, or operating condition, can affect the optimization of another. For example, supersaturation of the incoming gas streams results in a very high current density at the inlet but also the formation of liquid water (i.e., flooding), which lowers the performance owing to the increased film resistance for diffusion. By contrast, dry gas streams on either anode or cathode cause low membrane conductivity and low performance, so components must be chosen to retain water. Because there are so many interacting parameters that need to be optimized, it is not possible to test all possible combinations within a reasonable amount of time. Therefore, the MEA manufacturer relies heavily on statistical analysis to test those combinations that have the highest probability for success.

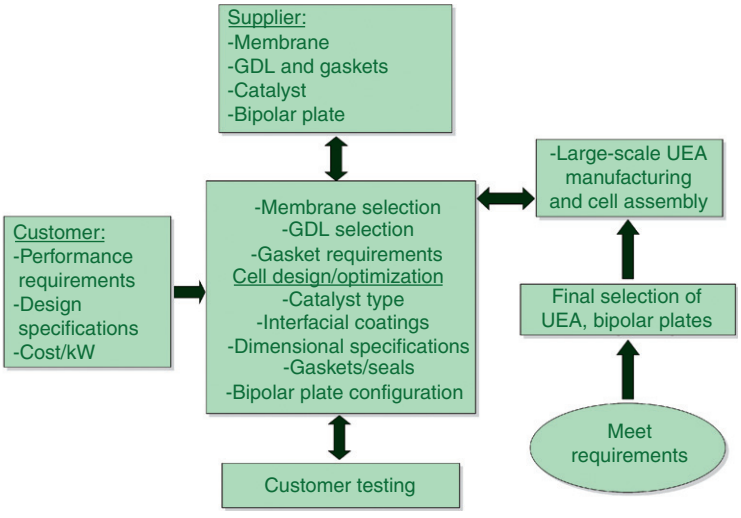


**Figure 6** A quality control flow sheet for selecting components toward proper cell design and manufacturing. GDL, gas diffusion layer; UEA, unitized electrode assembly.

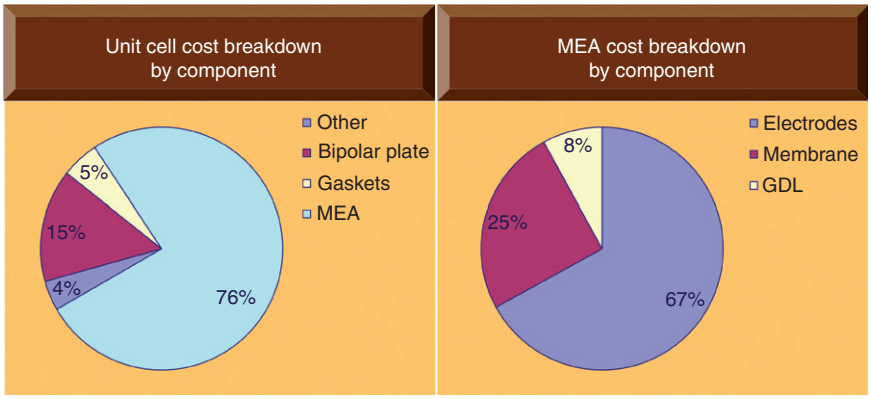


**Figure 7** Unit cell cost breakdown by individual components (left) and further breakdown of the membrane–electrode assembly (MEA) cost owing to membrane, electrode, and gas diffusion layer (GDL) (right). Note that this cost analysis takes into account certain design assumptions and material selections.

## Cell Development Challenges

Current challenges toward commercializing the PEMFC technology are (1) reducing the cost and (2) increasing the durability.

### Cost

The cost of the fuel cell module consisting of the fuel cell stack, air supply system, and coolant circulation system could amount to 50–60% of the overall cost of the fuel cell power plant. Among these, the cost of the fuel cell stack dominates (~80–85%) the fuel cell module cost. The cost distribution of the individual components of a unit cell is shown in Figure 7. The MEA with the precious metal catalyst and the PEM contribute to most of the cost of a unit cell. The current challenge in bringing down the cost of the MEA lies in the development of alternative membranes that are as functional and durable yet cheaper than Nafion and finding alternative nonprecious catalysts that have similar or more activity toward HOR and ORR.

### Durability

Although cost remains a main barricade on the road to PEMFC commercialization, durability targets also present significant challenges to design engineers. The exact degradation mechanism by which the PEMFCs fail has been delineated thanks to an explosion of durability-centered research in the first half of the first decade of twenty-first century. Proton-exchange membrane fuel cell degradation occurs owing to chemical and mechanical causes. Accelerated durability tests such as OCV decay (i.e., leaving a cell at open-circuit potential), load (or potential), humidity, and temperature (e.g., freeze–thaw) cycling routinely conducted as part of MEA/UEA performance evaluation indicate that the membrane loses its physical structure and disintegrates over a period of

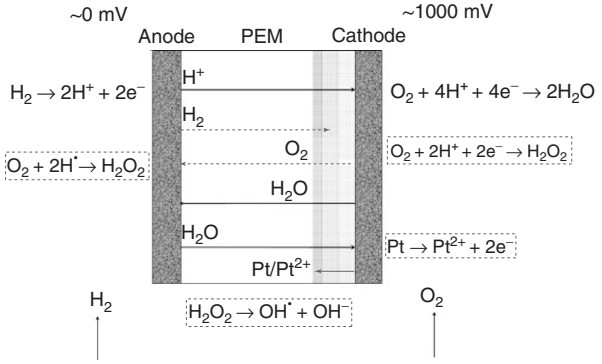


**Figure 8** Schematic of the membrane–electrode assembly (MEA) showing the important reactions and fluxes of key species in a proton exchange membrane (PEM) unit cell. The reactions in dashed boxes cause or contribute to membrane degradation and have important consequences toward proton-exchange membrane fuel cell (PEMFC) durability.

time. Drop in the cell potential, an increase in the hydrogen crossover current, and optical images of failed MEAs from these durability experiments indicate that membrane thinning and/or pinholes occur over a period of time. Figure 8 shows a schematic of reactant flows across a catalyst-coated membrane in a PEMFC unit cell. The presence of a very high potential (typical requirement for low-cost stack design) on the cathode causes platinum oxidation to platinum monoxide (PtO) and dissolution as $Pt^{2+}$. Both platinum monoxide and $Pt^{2+}$ migrate into the membrane because of concentration gradient. The $Pt^{2+}$ species in the membrane are reduced by molecular $H_2$ crossing over from the anode side resulting in chemical platinization of the membrane (i.e., $2Pt^{2+} + H_2 \rightarrow 2Pt + 2H^+$). Similar platinization of membranes has been shown to take place via chemical procedures for the metallization of membranes in which anionic metal ions in a solution in contact with one face of PEM are reduced by a reductant that diffuses through the membrane from a solution in contact with the

opposite face of the membrane. Also, a two-step impregnation–reduction method exists in which the membrane (e.g., Nafion) was ion-exchanged with a precursor metal salt followed by an exposure to a reductant. Similar chemical platinization occurs in a PEMFC membrane, where the $Pt^{2+}$ ions act as the source for platinum and hydrogen crossing over from the anode acts as a reductant. The chemical platinization occurs in the membrane at a distance $X_0$ from the cathode–membrane interface. This distance is dictated by the relative fluxes of molecular oxygen and hydrogen owing to diffusion from the cathode and anode sides, respectively. The lower potential on the anode side of the membrane together with oxygen crossing over from the cathode side drives the peroxide formation reaction. The peroxide thus formed disintegrates into $OH^{\bullet}$ radicals on the platinum in the membrane. The $OH^{\bullet}$ radicals thus formed attack the membrane and produce HF. Direct radical formation can also occur in that $OH^{\bullet}$ radicals are formed directly from the crossover of oxygen if favorable potentials exist. These phenomena are very sensitive to temperature and local water content. Increased temperatures and low humidity (both crucial requirements for automotive stacks) accelerate these degradation reactions, causing membrane failure and MEA degradation.

In addition to the above-described chemical degradation mechanism, routine mechanical stresses induced in a membrane owing to periodic swelling upon water uptake and thinning upon drying also cause failure. Therefore, the current cell development challenges include minimizing the cost without compromising the chemical and mechanical durability of the cell components.

## Main Applications

The first application of a PEMFC was in the 1960s as an auxiliary power source in the Gemini space flights. Subsequent advances in the PEMFC technology were stagnant until the 1980s when the fundamental design of the cell components underwent considerable reconfiguration. Since then, PEMFCs have been used for a number of applications and can be broadly classified into the following four areas: (1) automotive; (2) stationary power; (3) mobile units (such as electronic devices); and (4) military and space applications. The unit cells are typically assembled into stacks, which are then used as power modules in fuel cell power plants for these applications (see **Fuel Cells – Proton-Exchange Membrane Fuel Cells:** Stacks for an overview of the above-listed applications).

## Concluding Remarks

This article is an overview of its operational principle based on the functions of individual components. The current–voltage curve of a unit cell is discussed with respect to losses owing to kinetic, ohmic, and concentration polarizations. The current developmental challenges faced by the fuel cell community are in reducing the cost of the fuel cell components without sacrificing the performance and durability characteristics.

## Nomenclature

### Symbols and Units

| | |
|---|---|
| ***D*** | diameter |
| ***l*** | length or thickness |
| ***R*** | resistance |
| $\rho$ | specific resistance |

### Abbreviations and Acronyms

| | |
|---|---|
| **ACL** | anode catalyst layer |
| **CCL** | cathode catalyst layer |
| **DoE** | Department of Energy |
| **ECA** | electrochemical area |
| **EIS** | electrochemical impedance spectroscopy |
| **GDL** | gas diffusion layer |
| **HOR** | hydrogen oxidation reaction |
| **MEA** | membrane–electrode assembly |
| **OCV** | open-circuit voltage |
| **ORR** | oxygen reduction reaction |
| **PEM** | proton exchange membrane |
| **PEMFC** | proton-exchange membrane fuel cell |
| **PTFE** | polytetrafluoroethylene |
| **PTL** | porous transport layer |
| **RDE** | rotating disk electrode |
| **RH** | relative humidities |
| **UEA** | unitized electrode assembly |

*See also:* **Fuel Cells – Overview:** Introduction; Modeling; **Fuel Cells – Proton-Exchange Membrane Fuel Cells:** Anodes with Reformate; Bipolar Plates; Catalysts: Life-Limiting Considerations; Cathodes; Dynamic Operational Conditions; Gas Diffusion Layers; Membrane–Electrode Assemblies; Membrane: Life-Limiting Considerations; Membranes: Elevated Temperature; Overview Performance and Operational Conditions; Stacks; Systems; **History:** Fuel Cells.

## Further Reading

Barbir F (2006) PEM fuel cells. In: Sammes NS (ed.) *Fuel Cell Technology: Reaching Towards Commercialization*, pp. 27–51. London: Springer.

Bernardi DM and Verbrugge DM (1992) A mathematical model of the solid-polymer-electrolyte fuel cell. *Journal of the Electrochemical Society* 139: 2477–2491.

Berning T, Lu DM, and Djilali N (2002) Three-dimensional computational analysis of transport phenomena in a PEM fuel cell. *Journal of Power Sources* 106: 284–294.

Cleghorn SJC, Ren X, Springer TE, et al. (1997) PEM fuel cells for transportation and stationary power generation applications. *International Journal of Hydrogen Energy* 22: 1137–1144.

Costamagna P and Srinivasan S (2001a) Quantum jumps in the PEMFC science and technology from the 1960s to the year 2000: Part I. Fundamental scientific aspects. *Journal of Power Sources* 102: 242–252.

Costamagna P and Srinivasan S (2001b) Quantum jumps in the PEMFC science and technology from the 1960s to the year 2000: Part II. Engineering, technology development and application aspects. *Journal of Power Sources* 102: 253–269.

Dutta S, Shimpalee S, and Van Zee JW (2000) Three-dimensional numerical simulation of straight channel PEM fuel cells. *Journal of Applied Electrochemistry* 30: 135–146.

Dutta S, Shimpalee S, and Van Zee JW (2001) Numerical prediction of mass-exchange between cathode and anode channels in a PEM fuel cell. *International Journal of Heat and Mass Transfer* 44: 2029–2042.

EG&G Services (2004) *Fuel Cell Handbook,* 7th edn. Morgantown: United States Department of Energy.

Gasteiger HA, Kocha SS, Sompalli B, and Gottesfeld S (2000) Activity benchmarks and requirements for Pt, Pt-alloy, and non-Pt oxygen reduction catalysts for PEMFCs. *Applied Catalysis B: Environmental* 56: 9–35.

He W, Yi JS, and Nguyen TV (2000) Two-phase flow model of the cathode of PEM fuel cells using interdigitated flow fields. *AIChE Journal* 46: 2053–2064.

Hickner MA, Ghassemi H, Kim YS, Einsla BR, and McGrath JE (2004) Alternative polymer systems for proton exchange membranes (PEMs). *Chemical Reviews* 104: 4587–4611.

Kramer D, Zhang J, Shimoi R, Lehmann E, Wokaun A, Shinohara K, and Scherer GG (2005) In situ diagnostic of two-phase flow phenomena in polymer electrolyte fuel cells by neutron imaging: Part A. Experimental, data treatment, and quantification. *Electrochimica Acta* 50: 2603–2614.

Kreuer KD (2001) On the development of proton conducting polymer membranes for hydrogen and methanol fuel cells. *Journal of Membrane Science* 185: 29–39.

Mathias MF, Makharia R, Gasteiger HA, et al. (2005) Two fuel cell cars in every garage? *Electrochemical Society Interface* 14: 24–35.

Mench MM (2008) *Fuel Cell Engines*. Hoboken, NJ: John Wiley & Sons Inc.

Mench MM, Dong QL, and Wang CY (2003) In situ water distribution measurements in a polymer electrolyte fuel cell. *Journal of Power Sources* 124: 90–98.

Mench MM, Wang CY, and Ishikawa M (2003) In situ current distribution measurements in polymer electrolyte fuel cells. *Journal of the Electrochemical Society* 150: A1052–A1059.

Meyers JP and Maynard HL (2002) Design considerations for miniaturized PEM fuel cells. *Journal of Power Sources* 109: 76–88.

Natarajan D and Nguyen TV (2001) A two-dimensional two-phase, multicomponent transient model for the cathode of a proton exchange membrane fuel cell using conventional gas distributors. *Journal of the Electrochemical Society* 148: A1324–A1335.

Pasaogullari U and Wang CY (2004) Liquid water transport in gas diffusion layer of polymer electrolyte fuel cells. *Journal of the Electrochemical Society* 151: A399–A406.

Rolison DR (2003) Catalytic nanoarchitectures – the importance of nothing and the unimportance of periodicity. *Science* 299: 1698–1701.

Shimpalee S and Dutta S (2000) Numerical prediction of temperature distribution in PEM fuel cells. *Numerical Heat Transfer; Part A: Applications* 38: 111–128.

Springer TE, Zawodzinski TA, and Gottesfeld S (1991) Polymer electrolyte fuel cell model. *Journal of the Electrochemical Society* 138: 2334–2342.

Steele BCH and Heinzel A (2001) Materials for fuel-cell technologies. *Nature* 414: 345–352.

Wang CY (2004) Fundamental models for fuel cell engineering. *Chemical Reviews* 104: 4727–4765.

Wang H, Sweikart MA, and Turner JA (2003) Stainless steel as bipolar plate material for polymer electrolyte membrane fuel cells. *Journal of Power Sources* 115: 243–251.

Wang ZH, Wang CY, and Chen KS (2001) Two-phase flow and transport in the air cathode of proton exchange membrane fuel cells. *Journal of Power Sources* 94: 40–50.

Weber AZ and Newman J (2004) Modeling transport in polymer-electrolyte fuel cells. *Chemical Reviews* 104: 4679–4726.

Yi JS and Nguyen TV (1998) An along-the-channel model for proton exchange membrane fuel cells. *Journal of the Electrochemical Society* 145: 1149–1159.

Zawodzinski TA, Derouin C, Radzinski S, Sherman RJ, Smith VT, Springer TE, and Gottesfeld S (1993) Water uptake by and transport through Nafion® 117 membranes. *Journal of the Electrochemical Society* 140: 1041–1047.

Zhang FY, Yang XG, and Wang CY (2006) Liquid water removal from a polymer electrolyte fuel cell. *Journal of the Electrochemical Society* 153: A225–A232.